8668 *Inorg. Chem.* **2009**, *48*, 8668–8677
DOI: 10.1021/ic900780a

Inorganic Chemistry
Article

Copolymerization of Epoxides and Carbon Dioxide. Evidence Supporting the Lack of Dual Catalysis at a Single Metal Site

Donald J. Darensbourg* and Shawn B. Fitch

Department of Chemistry, Texas A&M University, College Station, Texas 77843

Received April 22, 2009

The chromium tetramethyltetraazaannulene catalyst system, Cr(tmtaa)Cl in the presence of a quaternary organic salt, has been employed to further investigate the mechanism of polycarbonate formation between cyclohexene oxide and carbon dioxide. Although the features of the proposed mechanism are generally well-accepted, the question of whether polymer chain propagation occurs from one side of the catalyst in a mono catalytic single-site fashion or from both sides of the N_4-ligand plane in a dual catalytic manner. To probe this behavior, the ligand architecture was altered by the addition of a sterically encumbering strap (Cr(stmtaa)Cl), which effectively blocks one side of the complex and limits polymer chain growth to a single side of the catalyst. For direct comparison, an electronically similar catalyst, Cr(s^{m}tmtaa)Cl, was prepared to mimic the strap complex while not possessing the site-blocking steric restraints of the full strap. Infrared spectroscopy demonstrated an uptake of 2 equiv of $PPNN_3$ cocatalyst by the strap mimic catalyst, while only 1 equiv of azide was able to bind to the catalyst containing the full strap, supporting the design function of both complexes. Monitoring the formation of poly(cyclohexylene carbonate) from the reaction of cyclohexene oxide and carbon dioxide via in situ infrared spectroscopy for both Cr(stmtaa)Cl and Cr(s^{m}tmtaa)Cl, under identical conditions, revealed copolymer formation at essentially equivalent rates. Analysis of the polycarbonate products found that Cr(stmtaa)Cl and Cr(s^{m}tmtaa)Cl produced copolymers with turnover frequencies of 806.6 and 797.3 h^{-1}, molecular weights of 11,431 and 12,003 Da, and polydispersities of 1.108 and 1.048, respectively. These results strongly support the idea that this and other catalysts systems presumed to operate by a similar process, such as Cr(salen)X, catalyze the copolymerization of epoxides with carbon dioxide through a mono catalytic single-site mechanism.

Introduction

The production of polymeric materials, specifically polycarbonates, from the coupling of epoxides and carbon dioxide represents a viable technological use of carbon dioxide, as both a monomer and a solvent (eq 1). Since the pioneering work of Inoue and co-workers, which demonstrated the feasibly of forming polycarbonates from CO_2 and aliphatic epoxides, this area of chemistry has flourished worldwide.[1] Prominent among studies over the last 15 years are the development of discrete metal complexes, which serve as very effective catalysts for these processes, based on both main group and transition metals.[2]

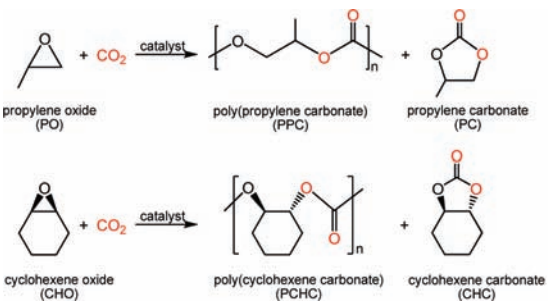

(1)

One of the most widely studied catalytic systems utilizes a salen-based architecture with a chromium metal center and was inspired by the work of Jacobsen and co-workers.[3,4] The chromium salen system (Figure 1) has been modified to adjust electronic and steric properties, examined with

*To whom correspondence should be addressed. E-mail: djdarens@mail.chem.tamu.edu. Fax: (979) 845-0158.

(1) (a) Inoue, S.; Koinuma, H.; Tsuruta, T. *J. Polym. Sci., Part B* **1969**, *7*, 287–292. (b) Inoue, S.; Koinuma, H.; Tsuruta, T. *Makromol. Chem.* **1969**, *130*, 210–220.

(2) (a) Coates, G. W.; Moore, D. R. *Angew. Chem., Int. Ed.* **2004**, *43*, 6618–6639. (b) Darensbourg, D. J. *Chem. Rev.* **2007**, *107*, 2388–2410.

(3) Hansen, K. B.; Leighton, J. L.; Jacobsen, E. N. *J. Am. Chem. Soc.* **1996**, *118*, 10924–10925.

(4) Jacobsen, E. N. *Acc. Chem. Res.* **2000**, *33*, 421–431.

Published on Web 06/19/2009

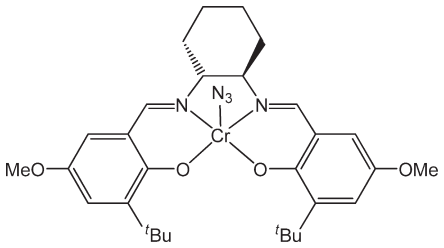

Figure 1. Skeletal representation of a chromium salen catalyst used for the copolymerization of epoxide and carbon dioxide.

various nucleophilic cocatalysts, and a mechanism has been proposed for the copolymerization reaction.[5−15] The reaction pathway, shown in Figure 2, begins by the addition of a nucleophilic cocatalyst. This anionic complex initiates the polymerization by ring-opening an incoming activated epoxide molecule. Carbon dioxide is inserted into the chromium alkoxide bond in the absence of prior coordination to the metal center, resulting in the formation of a carbonate linkage. The catalytic cycle is continued by the alternating ring-opening of epoxide and insertion of carbon dioxide.

It is important to note that both nucleophiles (Nu or X) can serve as initiators. Indeed, for a given copolymerization process both Nu and X have been observed as end groups on the thus afforded copolymers.[2b] This process is further complicated by the fact that we have demonstrated that when Nu≠X, ligand redistribution reactions can occur. For example, (salen)CrCl in the presence of 1 equiv of azide ions exists in solution as a mixture of (salen)$CrCl_2^-$, (salen)Cr-$(N_3)_2^-$, and (salen)Cr$(N_3)Cl^-$ complexes.[15] Nevertheless, these observations do not necessitate *simultaneous* polymer growth from both sides of the —Cr— plane as depicted in a more comprehensive scheme as outline in Figure 3, and this issue remains an ambiguity of the copolymerization mechanism. That is, in general the observed molecular weights of the copolymers are much less than anticipated from the calculated molecular weights based on the monomer/initiator ratio and % conversion for a single site catalyst. This discrepancy in calculated and theoretical molecular weights can arise from a monomer/initiator ratio that is half as large for the double-sided pathway (right side Figure 3) as the single-sided polymer growth pathway (left side of Figure 3), or chain-transfer reactions involving adventitious water. Previous reports studying epoxide/CO_2 copolymerizations using aluminum-, chromium-, and cobalt porphyrin and salen catalysts have proposed that these complexes are dicatalytic single-site catalysts, where polymer chain growth occurs from both sides of the metal center, while others support chain growth from only one side.[16−21] In either instance, a lack of control of the copolymer's molecular weight can result from chain transfer reactions from trace water.

A more highly active metal catalyst for the copolymerization of cyclohexene oxide and CO_2 incorporates the tetramethyltetraazaannulene (tmtaa) macrocyclic ligand architecture. That is, the chromium complex, Cr(tmtaa)Cl (**1**), has been shown to achieve activities of 1500 turnovers per hour (turnover frequency, TOF = mole epoxide consumed per mole catalyst per hour) while suppressing the formation of cyclic cyclohexene carbonate, concomitantly producing polycyclohexylene carbonate at moderate molecular weights with high CO_2 incorporation and narrow polydispersities.[21,22] Investigations into the mechanistic aspects of the chromium tetramethyltetraazaannulene catalyst system suggest a similar pathway for copolymerization of epoxides and carbon dioxide as proposed for the chromium salen catalysts. This has allowed for a direct comparison between these two closely related systems. Nevertheless, it is noteworthy that tetramethyltetraazaannulene complexes do not exhibit the relative ligand planarity inherent to salen and porphyrin complexes, but rather possesses a well pronounced saddle shape (Figure 4).

Following the work of Sakata and co-workers,[23] opposing sides of the tetramethyltetraazaannulene ligand have been tethered via a strap running beneath the ligand (Figure 5). This added steric bulk should limit catalytic activity to only one side of the complex, while leaving enough space on the tethered side for the necessary binding of a small anion. If this hypothesis is correct, the chromium tmtaa catalyst featuring the strap moiety, Cr(stmtaa)Cl (**2**), would exhibit similar catalytic activity as observed for the unmodified catalyst, Cr-(tmtaa)Cl, while producing a copolymer with similar constitution if polymer propagation occurs from only one side of the metal center.

Experimental Section

Methods and Materials. Unless otherwise specified, all manipulations were carried out on a double manifold Schlenk vacuum line under an atmosphere of argon or in an argon-filled glovebox. Methanol (EMD Chemicals), absolute ethanol (Pharmco-Aaper), 2,4-pentanedione (Aldrich), nickel acetate tetrahydrate (Fisher), chromium(III) chloride (Strem), ammonium hexafluorophosphate (Oakwood), sodium azide (Aldrich), sodium chloride (EMD Chemicals), sodium cyanate (Aldrich), sodium cyanide (Aldrich), potassium hydroxide (EMD Chemicals), *N*,*N*-dimethylformamide (Aldrich), 3-hydroxybenzoic acid (Alfa Aesar), *m*-anisic acid (Alfa Aesar),

(5) Darensbourg, D. J.; Wildeson, J. R.; Lewis, S. J.; Yarbrough, J. C. *J. Am. Chem. Soc.* **2002**, *124*, 7075–7083.
(6) Darensbourg, D. J.; Yarbrough, J. C. *J. Am. Chem. Soc.* **2002**, *124*, 6335–6342.
(7) Darensbourg, D. J.; Rodgers, J. L.; Fang, C. C. *Inorg. Chem.* **2003**, *42*, 4498–4500.
(8) Darensbourg, D. J.; Yarbrough, J. C.; Ortiz, C.; Fang, C. C. *J. Am. Chem. Soc.* **2003**, *125*, 7586–7591.
(9) Darensbourg, D. J.; Mackiewicz, R. M.; Phelps, A. L.; Billodeaux, D. R. *Acc. Chem. Res.* **2004**, *37*, 836–844.
(10) Darensbourg, D. J.; Mackiewicz, R. M.; Rodgers, J. L.; Fang, C. C.; Billodeaux, D. R.; Reibenspies, J. H. *Inorg. Chem.* **2004**, *43*, 6024–6034.
(11) Darensbourg, D. J.; Mackiewicz, R. M.; Rodgers, J. L.; Phelps, A. L. *Inorg. Chem.* **2004**, *43*, 1831–1833.
(12) Darensbourg, D. J.; Mackiewicz, R. M. *J. Am. Chem. Soc.* **2005**, *127*, 14026–14038.
(13) Darensbourg, D. J.; Bottarelli, P.; Andreatta, J. R. *Macromolecules* **2007**, *40*, 7727–7729.
(14) Darensbourg, D. J.; Frantz, E. B. *Inorg. Chem.* **2007**, *46*, 5967–5978.
(15) Darensbourg, D. J.; Moncada, A. I. *Inorg. Chem.* **2008**, *47*, 10000–10008.
(16) Aida, T.; Ishikawa, M.; Inoue, S. *Macromolecules* **1986**, *19*, 8–13.
(17) Sugimoto, H.; Ohtsuka, H.; Inoue, S. *J. Polym. Sci., Part A: Polym. Chem.* **2005**, *43*, 4172–4186.
(18) Nakano, K.; Kamada, T.; Nozaki, K. *Angew. Chem., Int. Ed.* **2006**, *45*, 7274–7277.
(19) Qin, Y.; Wang, X.; Zhang, S.; Zhao, X.; Wang, F. *J. Polym. Sci., Part A: Polym. Chem.* **2008**, *46*, 5959–5967.
(20) Cohen, C. T.; Chu, T.; Coates, G. W. *J. Am. Chem. Soc.* **2005**, *127*, 10869–10878.
(21) Darensbourg, D. J.; Fitch, S. B. *Inorg. Chem.* **2007**, *46*, 5474–5476.
(22) Darensbourg, D. J.; Fitch, S. B. *Inorg. Chem.* **2008**, *47*, 11868–11878.
(23) Sakata, K.; Ueno, A.; Jibuta, T.; Hashimoto, M. *Synth. React. Inorg., Met.-Org., Chem.* **1993**, *23*, 1107–1115.

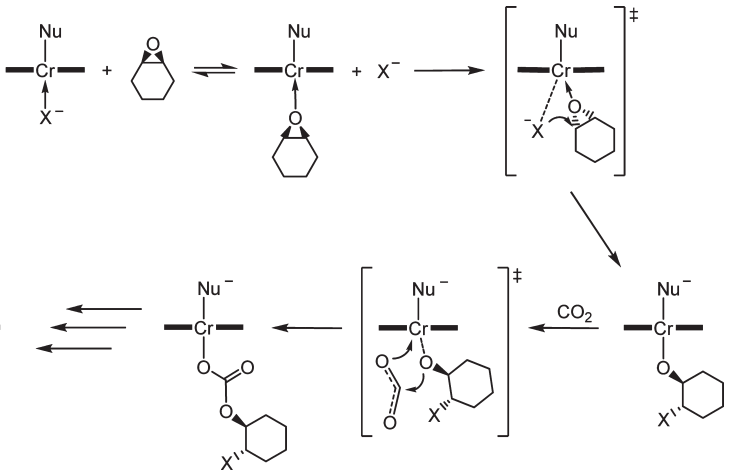

Figure 2. Proposed mechanism for the chromium salen catalyzed copolymerization of cyclohexene oxide and carbon dioxide.

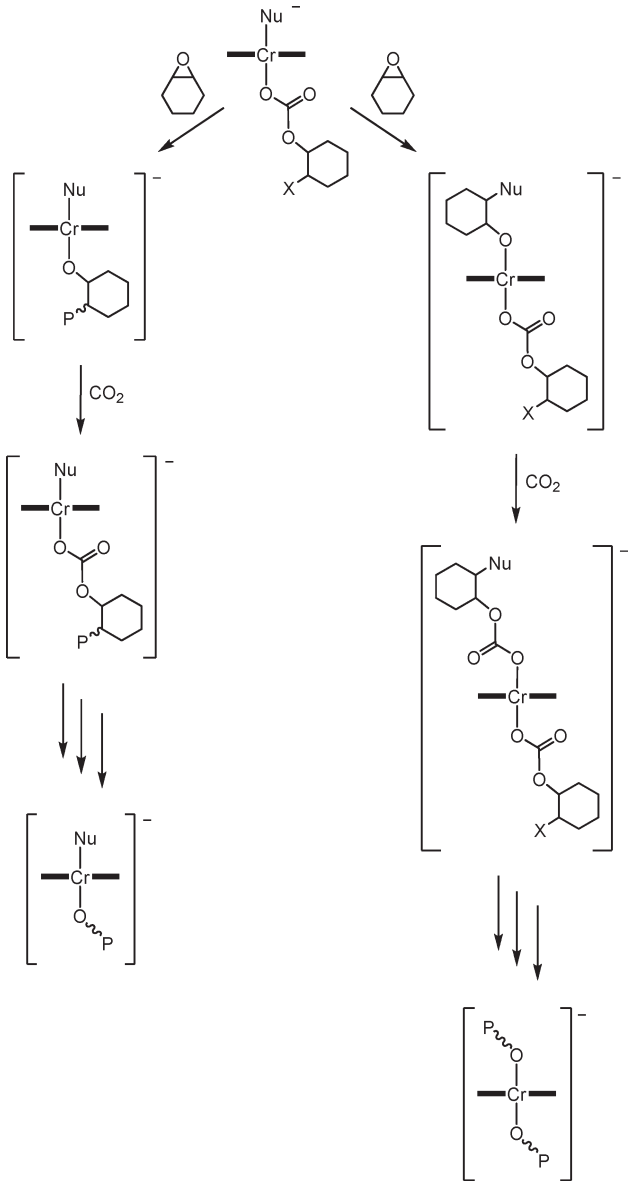

Figure 3. Proposed mechanisms for one-sided monomer insertion (left) vs monomer insertion occurring on both sides of the chromium catalyst (right).

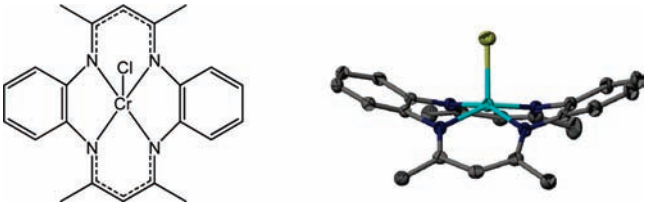

Figure 4. Skeletal (left) and three-dimensional (right) representations of complex **1** used to catalyze the copolymerization of epoxides and carbon dioxide.

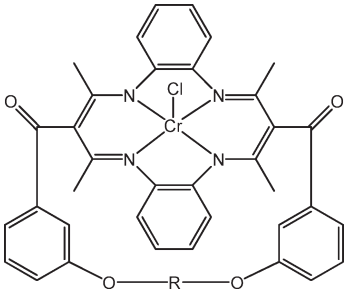

Figure 5. Skeletal representation of a strapped chromium tetramethyltetraazaannulene complex, where R = an alkyl or aromatic linker.

m-xylene dibromide (Alfa Aesar), 1,6-dibromohexane (Acros), methyl 3-hydroxybenzoate (Alfa Aesar), sodium hydride (Alfa Aesar), sulfuric acid (EMD Chemicals), and hydrochloric acid (EMD Chemicals) were used without further purification. Triethylamine (EMD Chemicals) was stored over sodium hydroxide and freshly distilled before use. Thionyl chloride (Aldrich) was distilled prior to use. Bis(triphenylphosphoranylidene)ammonium chloride was recrystallized from methylene chloride/ether. Bis(triphenylphosphoranylidene)-ammonium azide was synthesized from a published literature procedure.[24] Methylene chloride, benzene, hexane, tetrahydrofuran, methanol, ethyl ether, and toluene were freshly purified by an MBraun Manual Solvent System packed with Alcoa F200 activated alumina desiccant. The synthesis of H_2tmtaa was conducted following published procedures.[25] Cyclohexene oxide (TCI) was freshly distilled from CaH_2 (Alfa Aesar) prior to use. Acetone (Pharmco-Aaper) was freshly distilled from sodium carbonate (EMD Chemicals)

(24) Demadis, K. D.; Meyer, T. J.; White, P. S. *Inorg. Chem.* **1998**, *37*, 3610–3619.
(25) Goedken, V. L.; Weiss, M. C. *Inorg. Synth.* **1980**, *20*, 115.

prior to use. Bone dry carbon dioxide (Scott Specialty Gases) was supplied in a high pressure cylinder equipped with a liquid dip-tube. Unless otherwise stated, all other reagents were used without further purification. ^{1}H and ^{13}C NMR spectra were acquired using a Varian Inova 300 or 500 MHz superconducting NMR spectrometers. Infrared spectra were recorded on a Bruker Tensor 27 FTIR spectrometer. Molecular weight determinations were carried out on a Viscotek Gel Permeation Chromatograph equipped with refractive index, right-angle and low-angle light scattering detectors.

Synthesis of 3,3′-(1,3-Phenylenebis(methylene))bis(oxy)dibenzoic Acid. The synthesis was conducted through modification of a reported procedure.[26] A 4 g portion (26.3 mmol) of methyl 3-hydroxybenzoate was dissolved in 20 mL of tetrahydrofuran (THF) and added to a slurry of 0.63 g (26.3 mmol) NaH in 10 mL of THF. After hydrogen gas evolution had ceased, the clear solution was allowed to stir for an additional 20 min. The solvent was removed under reduced pressure, and the residue dissolved in 40 mL of dry DMF. A 3.47 g portion (13.15 mol) of *m*-xylene dibromide was added, and the solution refluxed for 10−15 min. The DMF was removed under reduced pressure, and the tan residue dissolved in a minimal amount of acetone and filtered to remove the precipitated NaBr. The solvent was removed in vacuo, and the residue refluxed in 70 mL of 10% KOH solution overnight. The solution was cooled, and the product precipitated as a white solid upon the addition of 40 mL of 6 N HCl. The precipitate was isolated, washed with water, and recrystallized from hot ethanol. Yield: 3.95 g (79.4%). ^{1}H NMR (*d*-DMSO, 300 MHz): δ 7.56−7.23 (m, 12H), 5.17 (s, 4H). ^{13}C{^{1}H} NMR (*d*-DMSO, 300 MHz): δ 167.09, 158.29, 137.09, 132.27, 129.74, 128.62, 127.22, 126.83, 121.82, 119.66, 114.90, 69.23.

Synthesis of 3,3′-(Hexane-1,6-diylbis(oxy))dibenzoic Acid. The synthesis was conducted by modifying a published procedure.[26] The same procedure outlined above was used with the substitution of 3.2 g (13.14 mmol) 1,6-dibromohexane in place of *m*-xylene dibromide. Yield: 3.15 g (67%). ^{1}H NMR (*d*-DMSO, 300 MHz): δ 7.51−7.15 (m, 8H), 4.01 (t, 4H), 1.74 (p, 4H), 1.48 (p, 4H). ^{13}C{^{1}H} NMR (*d*-DMSO, 300 MHz): δ 167.13, 158.62, 132.13, 129.68, 121.42, 119.34, 114.41, 67.55, 28.54, 25.23.

Synthesis of 5,14-Dihydro-6,8,15,17-tetramethyl-7,16-(3,3′-(2,6-phenylenedimethylenedioxydibenzoylo)dibenzo[b,i][1,4,8,11]tetraazacyclotetradecine (3). This synthesis was modified from a previous report.[23] A 1.2 g portion (3.18 mmol) of 3,3′-(1,3-phenylenebis(methylene))bis(oxy)dibenzoic acid was refluxed in 20 mL of thionyl chloride overnight. The thionyl chloride was removed under reduced pressure, the residue dissolved in 20 mL of benzene, and benzene was removed under reduced pressure to eliminate any remaining thionyl chloride. This benzene wash was repeated once more, and the residue dissolved in 1800 mL of toluene. A 1.1 g portion (3.19 mol) of H_2tmtaa and 4.5 mL (32.29 mmol) of NEt_3 were added, and the solution refluxed for 7 days. The solution was concentrated, filtered through Celite to remove triethylamine hydrochloride, and evaporated under reduced pressure. The product was purified by column chromatography over silica gel using dichloromethane as an eluent, collecting the second fraction. Removal of solvent yielded 1.49 g (68% yield) of pure product. X-ray quality crystals were obtained through slow evaporation of a chloroform solution. ^{1}H ($CDCl_3$, 500 MHz): δ 14.34 (s, 2H), 8.07 (s, 1H), 7.81 (t, 2H), 7.77 (d, 2H), 7.52 (t, 2H), 7.36 (t, 1H), 7.23 (m, 4H), 7.00 (m, 8H), 5.14 (s, 4H), 2.13 (s, 12H). ^{13}C{^{1}H} ($CDCl_3$, 500 MHz): δ 201.03, 158.51, 141.78, 137.26, 137.07, 130.18, 128.44, 126.18, 123.82, 123.79, 123.40, 120.73, 120.09, 115.60, 109.84, 69.58, 19.89.

Synthesis of 5,14-Dihydro-6,8,15,17-tetramethyl-7,16-(3,3′-hexamethylenedioxydibenzoylo)dibenzo[b,i][1,4,8,11]tetraazacyclotetradecine (H_2stmtaa, 4). The synthesis was conducted by modifying published procedures[23,27] and follows the procedure outlined above for compound **3** using 1.0 g (2.79 mmol) of 3,3′-(hexane-1,6-diylbis(oxy))dibenzoic acid in place of 3,3′-(1,3-phenylenebis(methylene))bis(oxy)dibenzoic acid. Yield: 1.02 g (55%). X-ray quality crystals were obtained through slow evaporation of a chloroform solution. ^{1}H NMR ($CDCl_3$, 500 MHz): δ 14.36 (s, 2H), 7.66 (d, 2H), 7.54 (s, 2H), 7.42 (t, 2H), 7.05 (d, 2H), 7.01 (s, 8H), 4.02 (t, 4H), 2.13 (s, 12H), 1.81 (p, 4H), 1.62 (p, 4H). ^{13}C{^{1}H} ($CDCl_3$, 500 MHz): δ 199.88, 159.81, 159.06, 142.21, 137.16, 130.04, 124.03, 123.62, 120.64, 117.60, 117.23, 110.23, 68.19, 28.66, 25.98, 20.28.

Synthesis of 5,14-Dihydro-6,8,15,17-tetramethyl-7,16-bis((3-methoxyphenyl)methanone)dibenzo[b,i][1,4,8,11]tetraazacyclotetradecine (H_2s^{m}tmtaa, 5). Modifying a previously reported procedure,[28] 6 g (15 mmol) of Ni(tmtaa) was dissolved in 100 mL of benzene, and 7 mL (50.2 mmol) of triethylamine. *m*-anisoyl chloride (5.12 g, 30 mmol) was added and the solution refluxed for 1.5−2 h and allowed to stand at room temperature overnight. The solvent was removed under reduced pressure, and the residue washed with hot water, isolated, and dried in vacuo. The neutral disubstituted ligand was obtained by bubbling anhydrous hydrogen chloride gas through the suspension of the crude nickel complex in dry acetone with vigorous stirring. Over the course of 2 h, an orange/yellow precipitate formed, and the solution was stirred overnight. The precipitate was isolated, washed with acetone, and dried. The collected material was returned to a flask and stirred vigorously with cold dilute (1:10) hydrochloric acid, filtered and washed with hot water followed by acetone to remove nickel chloride and the hydrochloride salt of the unsubstituted and monosubstituted ligands. The isolated γ,γ'-disubstituted hydrochloride ligand salt was transferred to a flask, dissolved in methanol, and neutralized by addition of excess triethylamine, resulting in precipitation of the pure, light green product. Yield: 4.317 g (47%). X-ray quality crystals were obtained through slow evaporation of a dichloromethane solution. MS (ESI): m/z 613.27 (M+H). ^{1}H NMR ($CDCl_3$, 300 MHz): δ 14.27 (s, 2H), 7.61 (d, 2H), 7.56 (s, 2H), 7.42 (t, 2H), 7.14−7.00 (m, 10H), 3.88 (s, 6H), 1.99 (s, 12H). ^{13}C{^{1}H} ($CDCl_3$, 300 MHz): δ 198.63, 160.81, 159.99, 142.44, 137.59, 129.75, 124.31, 122.57, 119.46, 112.84, 109.22, 109.00, 55.48, 19.28.

Synthesis of 5,14-Dihydro-6,8,15,17-tetramethyl-7,16-(3,3′-hexamethylenedioxydibenzoylo)dibenzo[b,i][1,4,8,11]tetraazacyclotetradecinato Chromium Chloride (Cr(stmtaa)Cl, 2). The chromium complex was synthesized following the procedure reported by Cotton for Cr(tmtaa)Cl (**1**).[29] A 1.07 g portion (1.61 mmol) of compound **4** was refluxed in 400 mL of benzene for 2 weeks in the presence of 1 equiv anhydrous chromium(III) chloride (0.255 g, 1.61 mmol) and 2 equiv (0.5 mL, 3.6 mmol) of freshly distilled triethylamine. Over the course of the reaction, the solution turned from yellow to burgundy, after which, the solution was filtered hot to remove triethylammonium chloride and concentrated under reduced pressure. The crude product was precipitated upon addition of hexanes, allowed to settle, and the supernatant decanted. This recrystallization procedure was repeated with dichloromethane/hexanes until the supernatant remained colorless. The product was dried in vacuo and stored in an argon-filled glovebox until use. Yield: 0.269 g (22%). X-ray quality crystals were obtained from a standing solution of DMSO. Anal. Calcd (%) for $C_{42}H_{40}ClCrN_4O_4\cdot 6H_2O$: C, 59.89; H, 5.98; N, 6.65; found: C, 59.77; H, 5.98; N, 6.63.

Synthesis of 5,14-Dihydro-6,8,15,17-tetramethyl-7,16-bis((3-methoxyphenyl)methanone)dibenzo[b,i][1,4,8,11]tetraazacyclotetradecinato Chromium Chloride (Cr(s^{m}tmtaa)Cl, 6). The chromium

(26) Elwahy, A. H. M.; Abbas, A. A. *Tetrahedron* **2000**, *56*, 885–895.

(27) Sakata, K.; Saitoh, Y.; Kawakami, K.; Nakamura, N.; Hashimoto, M. *Synth. React. Inorg., Met.-Org., Chem.* **1995**, *25*, 1279–1293.

(28) Eilmes, J. *Polyhedron* **1985**, *4*, 943–946.

(29) Cotton, F. A.; Czuchajowska, J.; Falvello, L. R.; Feng, X. *Inorg. Chim. Acta* **1990**, *172*, 135–136.

Table 1. Crystal Data and Structure Refinement for Compounds **3**, **4**, and **5**

	3·$CHCl_3$	H_2stmtaa·(**4**) 4$CHCl_3$	H_2s^mtmtaa (**5**)
empirical formula	$C_{45}H_{39}Cl_3N_4O_4$	$C_{46}H_{46}Cl12N_4O_4$	$C_{38}H_{36}N_4O_4$
formula wt, g/mol	806.15	1144.27	612.71
temp (K)	110(2)	110(2)	210(2)
wavelength (Å)	0.71073	0.71073	0.71073
crystal system	monoclinic	monoclinic	monoclinic
space group	$P2_1/n$	$P2_1/c$	$P2_1/c$
a (Å)	12.699(3)	11.8052(14)	11.039(7)
b (Å)	22.317(5)	18.600(2)	20.966(13)
c (Å)	14.771(4)	22.863(3)	14.447(9)
α (deg)	90	90	90
β (deg)	110.666(3)	97.3580(10)	109.086(11)
γ (deg)	90	90	90
cell volume (Å^3)	3917.0(16)	4978.7(10)	3160(3)
Z	4	6	4
density (calcd)	1.386	2.290	1.288
absorb coeff (mm^{-1})	0.285	1.073	0.085
obsd no. of reflcns	34993	56833	26387
no. of unique reflcns ($I > 2\sigma$)	8634	11961	7163
GoF	1.000	1.000	1.000
R,[a] % [$I > 2\sigma$]	6.45	3.35	6.93
R_w,[a] % [I > 2σ]	12.04	8.57	14.33

[a] $R = \sum||F_o|-|F_c||/\sum|F_o|$. $R_w = \{\sum w(F_o^2 - F_c^2)^2/\sum w(F_o^2)^2\}^{1/2}$.

complex was synthesized following the procedure reported by Cotton for Cr(tmtaa)Cl (**1**).[29] A 1.1 g portion (1.8 mmol) of compound **3** was refluxed in 350 mL of benzene for 1 week in the presence of 1 equiv of anhydrous chromium(III) chloride (0.285 g, 1.8 mmol) and 2 equiv (0.5 mL, 3.6 mmol) of freshly distilled triethylamine. Over the course of the reaction, the solution turned from yellow to burgundy, after which, the solution was filtered hot to remove triethylammonium chloride and concentrated under reduced pressure. The crude product was precipitated upon addition of hexanes, allowed to settle overnight, and the supernatant decanted. While allowed to settle overnight, crystals of the unreacted ligand were found on the flask's sides. A minimal amount of dichloromethane was carefully added to the bottom of the flask to dissolve the product, which was transferred to another flask. This recrystallization procedure was repeated with dichloromethane/hexanes, dichloromethane/ether, and THF/ether until the unreacted ligand was no longer observed. The product was dried in vacuo and stored in an argon-filled glovebox until use. Yield: 0.169 g (13.4%). Anal. Calcd (%) for $C_{38}H_{34}ClCrN_4O_4 \cdot 2H_2O \cdot CH_2Cl_2$: C, 57.19; H, 4.92; N, 6.84; found: C, 56.89; H, 4.93; N, 7.67.

Copolymerization of Cyclohexene Oxide and Carbon Dioxide. High pressure measurements of the copolymerization processes were carried out using a stainless steel Parr autoclave modified with a SiComp window to allow for attenuated total reflectance infrared spectroscopy (ASI ReactIR 1000 in situ probe). The catalyst and cocatalyst were dissolved in 10 mL of dichloromethane, allowed to stir for 30 min, and then dried in vacuo. The "activated" catalyst/cocatalyst mixture was then dissolved in 20 mL of neat cyclohexene oxide and injected into the autoclave via injection port and cannula, after which a single 128-scan background spectrum was collected. The autoclave was then charged with 35 bar carbon dioxide and a single 128-scan spectrum was taken every 2 min during the reaction period. Profiles of the absorbances at 1750 cm^{-1} (polycarbonate) and 1810 cm^{-1} (cyclic carbonate) versus time were recorded after baseline correction. After cooling and venting of the autoclave, the reaction was extracted with dichloromethane. The solution was dried overnight under a stream of compressed air to remove excess dichloromethane. The polymer residue was then dissolved in a minimum amount of dichloromethane and slowly added to a stirred beaker containing a 1 M HCl methanolic solution to remove the catalyst and precipitate the polycarbonate product. The supernatant solution containing the catalyst, cyclic carbonate, and any remaining cyclohexene oxide was decanted and the purified polymer dried in vacuo overnight. The dried polymer was collected and weighed to determine yield and the corresponding TONs and TOFs. The polymers were analyzed by ^{1}H NMR where the amount of ether linkages was determined by integrating the peaks corresponding to the methine protons of polyether at ~3.45 ppm and polycarbonate at ~4.6 ppm. Molecular weight determinations were carried out on a Viscotek Gel Permeation Chromatograph equipped with refractive index, right-angle light scattering, and low-angle light scattering detectors.

X-ray Structure Studies. A Leica microscope, equipped with a polarizing filter, was used to identify suitable crystals from a sample of crystals of the same habit. The representative crystal was coated in a cryogenic protectant, such as paratone, and affixed to a nylon sample loop attached to a copper mounting pin. The mounted crystals were then placed in a cold nitrogen stream (Oxford) maintained at 110 or 293 K on either a Bruker SMART 1000, GADDS, or APEX 2 three circle goniometer. The X-ray data were collected on either a Bruker CCD, GADDS, or an APEX 2 diffractometer and covered more than a hemisphere of reciprocal space by a combination of three (or nine in the case of the GADDS) sets of exposures; each exposure set had a different φ angle for the crystal orientation and each exposure covered 0.3° in ω. Crystal data and details on collection parameters are given in Table 1. The crystal-to-detector distance was 5.0 cm for all crystals. Crystal decay was monitored by repeating the data collection for 50 initial frames at the end of the data set and analyzing the duplicate reflections and found to be negligible. The space group was determined based on systematic absences and intensity statistics.[30] The structure was solved by direct methods and refined by full matrix least-squares on F^2. All non-H atoms were refined with anisotropic displacement parameters. All H atoms attached to C and N atoms were placed in idealized positions and refined using a rigid model with aromatic C−H = 0.93 Å, methyl C−H = 0.96 Å, amine N−H = 0.86 Å and with fixed isotropic displacement parameters equal to 1.2 (1.5 for methyl H atoms) times the equivalent isotropic displacement parameter of the atom to which they are attached. The methyl groups were allowed to rotate about their local 3-fold axis during refinement.

For all structures: data reduction, SAINTPLUS (Bruker[30]); program used to solve structures, SHELXS (Sheldrick[31]); program

(30) *SAINT-Plus*, version 6.02; Bruker: Madison, WI, 1999.
(31) Sheldrick, G. *SHELXS-86*; Institut fur Anorganische Chemie der Universität Göttingen: Göttingen, Germany, 1986.

used to refine structures, SHELXL-97 (Sheldrick[32]); molecular graphics and preparation of material for publication, SHELXTL-Plus version 5.0 (Bruker[33]) and XSEED (Barbour[34]).

Results and Discussion

Utilizing different anionic initiators (Nu and X groups in Figure 3) for the copolymerization of epoxides and CO_2 in the presence of (salen)CrX or (tmtaa)CrX complexes significantly different rates of copolymer growth have been observed as detected by in situ infrared monitoring of these processes. Concomitantly, the turnover frequencies (TOFs) obtained from isolated copolymers emphasized that different anionic cocatalysts resulted in different catalytic activities, with azide and chloride anions providing the highest rates of copolymer production.[12,22] If polymer chain propagation occurs from both sides of the CrN_4 structure, the rates of polymer formation should be quite similar following initiation since both sides of the metal would contain identical substituents, exemplified by the mechanism shown on the right in Figure 3. This would infer that the only difference in the polymerization activities when different cocatalyst anions were used would be in the rate of the initial ring-opening step. This is certainly not the case as cyclohexene oxide and propylene oxide ring-opening occurs rapidly, even at ambient temperature.[10,15]

Other researchers have found support for polymer chain growth occurring from both sides of the metal $-N_4$ or $-N_2O_2$ plane through analysis of the produced polycarbonates by gel permeation chromatography.[16−20] The refractive index-monitored GPC profiles indicated a distinct bimodal distribution in the polymer chain population. In each case, the higher-molecular-weight copolymer was approximately twice as large as that of the lower-molecular-weight one. This was attributed to the presence of two active species; one with two active sites and a polymer growing in two directions, and the other which propagated from one active site. More recently, Inoue and co-workers have probed deeper into this facet of the mechanism by employing an ultraviolet-active nucleophile, occupying the fifth coordination site of an aluminum salen catalyst, as well as a quaternary ammonium salt cocatalyst containing the same ultraviolet-active functionality.[17] These studies revealed only one of the copolymers of the bimodal molecular weight distribution contained the ultraviolet-active end group. The results of the study were inconclusive in determining the nature of the RI bimodal molecular weight distribution. MALDI-TOF mass spectrometry revealed the presence of hydroxyl end groups, indicating the bimodal distribution was most likely a product of chain termination by trace water contamination, a well-known occurrence in this immortal copolymerization process. Nevertheless, a copolymer propagating from a dinuclear metal catalyst system was proposed. After drying the hygroscopic Et_4NOAc cocatalyst at 130 °C in vacuo, the corresponding obtained polymer exhibited a unimodal GPC profile with a very small shoulder on the higher molecular weight region. This phenomenon, also observed with the chromium salen and tmtaa systems using the more hydrophobic PPNX cocatalysts, further supports the theory of one directional polymer chain growth and illustrates the detrimental effect water plays on polymerization control.

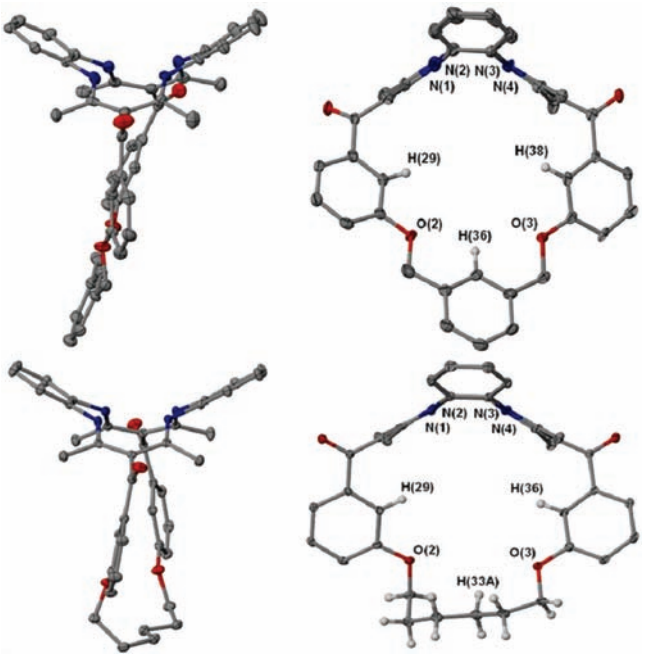

Figure 6. X-ray crystal structures of **3** (top) and **4** (bottom), showing both side-on and end-on perspectives. Thermal ellipsoids are shown at the 50% probability level with selected hydrogens and solvent molecules omitted for clarity.

Steric Approach to Mechanistic Elucidation. In an effort to investigate whether polymer chain growth occurs from one or both sides of the metal $-N_4$ plane, two ligands were synthesized with straps linking the γ and γ' methine carbons on the diiminato positions of the tmtaa ligand. These ligands were synthesized following or modifying the reports of Sakata and co-workers[23,27] and feature straps that allow enough space for the binding of a small anionic cocatalyst, but have sufficient steric bulk to block polymer growth. The solid state structures and crystallographic data of these ligands obtained by X-ray diffraction studies are shown in Figure 6 and Table 1. Solid state structures of **3** and **4** have previously been reported in the Cambridge Structural Database in 2005, but were refined with less accuracy and possessed a different unit cell for (**4**).[36,37] As illustrated, the two strapped ligands contain different linking groups that span the underside of the compound. The first, shown on the top, contains a *m*-xylylene group connecting the benzoyl functionalities on opposing sides of the ligand, with the second (bottom) being bridged by a more flexible hexylene chain. Table 2 lists distances of key atoms in the straps from the N_4 donor plane that illustrate the similar cavity sizes shared by the two ligands, where the closest contact is over 3.5 Å while the longest is 7.25 Å away from the nitrogen core.

It has been previously shown for both the chromium salen and the tmtaa systems that alteration of the electronic environment of the ligands by the addition of electron-withdrawing substituents resulted in diminished polymerization

(32) Sheldrick, G. *SHELXL-87*; Institut fur Anorganische Chemie der Universität Göttingen: Göttingen, Germany, 1987.
(33) *SHELXTL*, version 5.0; Bruker: Madison, WI, 1999.
(34) Barbour, L. J. *J. Supramol. Chem.* **2001**, *1*, 189–191.
(35) Inoue, S. *J. Polym. Sci., Part A: Polym. Chem.* **2000**, *38*, 2861–2871.
(36) Alcock, N. W.; Busch, D. H.; O'Brien, J. (**2005**) *Private communication to the Cambridge Structural Database, deposition number CCDC 286491.*
(37) Alcock, N. W.; Busch, D. H.; O'Brien, J. (**2005**) *Private communication to the Cambridge Structural Database, deposition number CCDC 286494.*

Table 2. Selected Contact Distances from the N_4 Donor Plane for **3** and **4**

	3 (Å)	H_2stmtaa (**4**) (Å)
N_4−H29	3.8401	3.5525
N_4−H36	6.5509	3.648
N_4−H38	3.5368	
N_4−O2	6.0389	5.938
N_4−O3	6.0074	6.1051
N_4−H33A		7.2520

activities.[10,22] The nature of the strapped complex is such that it is electronically unequal to the underivatized Cr(tmtaa)Cl complex and renders direct comparison invalid. To overcome this discrepancy, ligand alteration was needed that retained the electronic constraints of H_2stmtaa (**4**) without possessing its steric restrictions. Suitable ligand derivation was found upon reviewing the work of Eilmes and co-workers[28,38] and modified slightly to afford a strap "mimic" ligand, H_2s^mtmtaa (**5**), with an electronic environment that was comparable to **4**. As seen in Figure 7, complex **5** contains arms that exhibit rotational freedom, exemplified in the solid state structure where the arms are twisted to leave the underside of the ligand accessible, once metalated, to molecules associated with the copolymerization process. In support the rotational freedom of **5**, polymorphism has been observed and fully characterized in a similar complex.[39]

Cocatalyst Binding to Cr(stmtaa)Cl and Cr(s^mtmtaa)Cl. Synthesis of the corresponding chromium complexes of **4** and **5** was conducted following the reported procedure for complex **1** by Cotton and co-workers.[40] The hexylene-linked ligand, **4**, was chosen over that of the xylylene-linked, **3**, for metalation because of the greater flexibility in the strap and ease of synthesis.

Epoxide/CO_2 catalysts incorporating tetradentate ligand systems, such as porphyrin, salen, and tmtaa, require binding to occur at both of the ancillary sites to achieve high activity; therefore, complete blockage of one of these sites would not be beneficial. With that in mind, the strapped complex, Cr(stmtaa)Cl (**2**), and the corresponding strap mimic complex, Cr(s^mtmtaa)Cl (**6**), must not be so sterically encumbering to prevent the binding of a cocatalyst anion. To determine the catalysts' ability to bind cocatalyst, titrations were conducted in which sequential additions of $PPNN_3$ were added to complexes **2** and **6**, and the ν_{N3} vibrational mode was monitored by infrared spectroscopy. As can be seen from the overlay of infrared spectra for the addition of $PPNN_3$ to **2** in Figure 8, a metal-bound azide stretching band is observed at 2043 cm^{-1} with a high frequency shoulder. This band continues to grow in intensity until the [N_3^-] reaches 1 equiv. When the [N_3^-] reaches 1.5 equiv, the observance of a stretching band at 2005 cm^{-1}, corresponding to free N_3^- is apparent, indicating coordinative saturation of the chromium center after binding only 1 equiv of cocatalyst. From a previous cocatalyst binding study of complex **1**, the stretching band observed at 2043 cm^{-1} in Figure 8 corresponds to a six-coordinate chromium species. However, complex **1** was found to bind 2 equiv of N_3^- anion by displacing the originally bound chloride anion.[21] With these results, a proposed azide cocatalyst binding scheme is shown in Figure 9 where the sterically hindered underside of complex **2** is too encumbered to allow the azide anion access to the chromium center and instead, displaces the chloride ligand. Interpreting the observance of a six-coordinate chromium azide complex and only 1 equiv of azide uptake from Figure 8 suggests that the cavity is large enough to allow smaller ligands access to the metal center, such as the azide-displaced chloride, but restricting enough to impede the binding of the slightly larger azide anion.

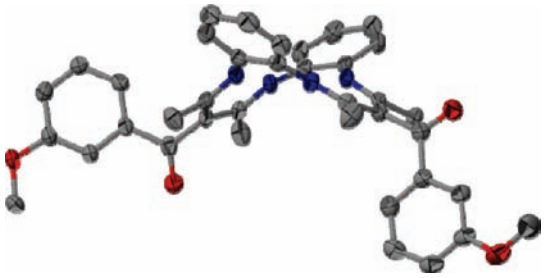

Figure 7. X-ray crystal structures of **5**, illustrating the flexibility of the anisoyl arms to expose the underside of the complex. Thermal ellipsoids are shown at the 50% probability level with hydrogens omitted for clarity.

Further support for selective access to the cavity of the strapped complex is provided by the solid state crystal structure (Table 3) obtained from a solution of DMSO, where the apical chloride has been displaced by a solvent molecule and recoordinated to the open site of the chromium center, within the strap cavity (Figure 10).

A comparison of **2** and **1** reveal little structural difference between the tetraazaannulene cores of the two complexes. As shown in Table 4 and illustrated in Figure 11 below, the coordination of DMSO trans to the chloride has increased the chromium-chloride bond length slightly. Interestingly, the out-of-plane distortion of the chromium from the nitrogen donor plane changed from 0.4235 Å above the plane in **1** to 0.0821 Å below the plane in **2**, concomitantly causing an enlargement in the chromium nitrogen bond angles. Also shown in Figure 11 are spheres representing the van der Waals radii of selected atoms to illustrate the steric allowances of the strap moiety. From the distances listed in Table 4, the closest contact to the chloride is 3.015 Å, well outside the sum of the van der Waals radii for hydrogen and chlorine of 2.84 Å, supporting the ability of a chloride anion from the required cocatalyst to bind to the chromium center within the steric confines of the strap.

To investigate the ability of complex **6**, acting as a strap mimic, to bind cocatalyst, a titration mirroring those previously completed for complexes **1** and **2** was conducted. Figure 12 shows an overlay of the infrared spectra of **6** as sequential amounts of $PPNN_3$ were added. As seen previously with **1**, as the [N_3^-] was increased, an absorbance band at 2043 cm^{-1} was observed, which grew in intensity until 2 equiv of N_3^- was reached. At [N_3^-] above 2 equiv, complex **6** became saturated with azide, apparent by the observance of an absorption band at 2005 cm^{-1}, indicative of free azide anion in solution. This study proves the strap mimic to behave, as predicted, like complex **1** rather than **2** and presumably retain the ability to undergo polymerization from both sides of the metal − N_4 plane, if necessary.

(38) Eilmes, J.; Ptaszek, M.; Zielinska, K. *Polyhedron* **2001**, *20*, 143–149.
(39) Sliwinski, J.; Eilmes, J.; Oleksyn, B. J.; Stadnicka, K. *J. Mol. Struct.* **2004**, *694*, 1–19.
(40) Cotton, F. A.; Czuchajowska, J. *Polyhedron* **1990**, *9*, 2553–2566.

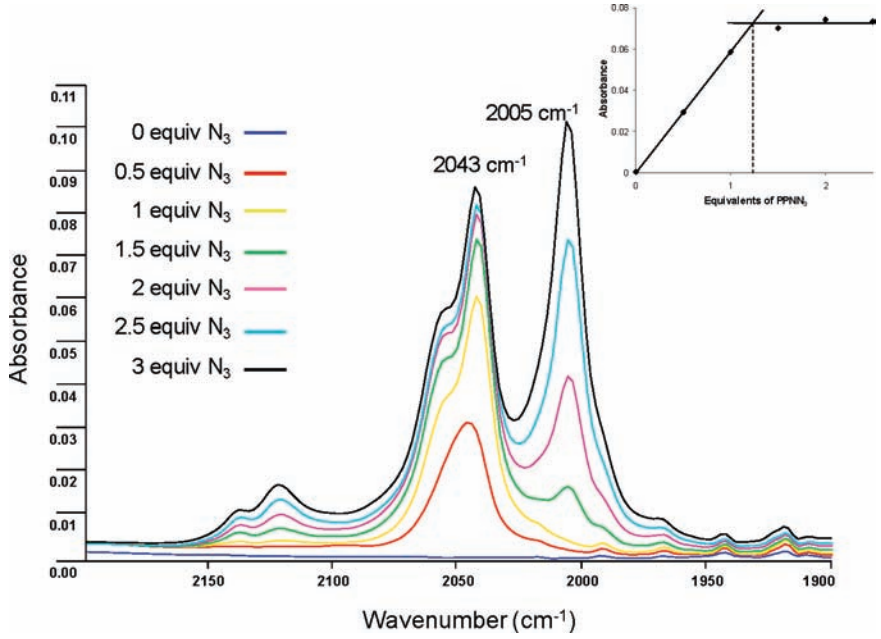

Figure 8. Infrared spectra from the titration of complex **2** with $PPNN_3$. Insert shows absorbance of ν_{N_3} band at 2043 cm^{-1} *vs* equivalents of $PPNN_3$.

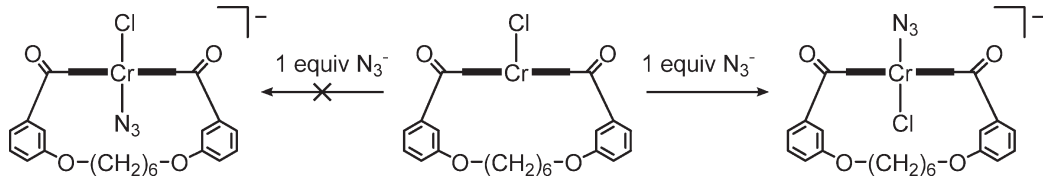

Figure 9. Proposed cocatalyst binding scheme between **2** and $PPNN_3$.

Table 3. Crystal Data and Structure Refinement for **2**

	Cr(stmtaa)Cl(DMSO)·1.5DMSO (**2**)
empirical formula	$C_{44}H_{46}ClCrN_4O_5S \cdot C_3H_9O_{1.5}S_{1.5}$
formula wt, g/mol	947.55
temp (K)	110(2)
wavelength (Å)	0.71073
crystal system	triclinic
space group	$P\bar{1}$
a (Å)	11.540(12)
b (Å)	12.128(13)
c (Å)	17.192(18)
α (deg)	75.31(2)
β (deg)	89.25(2)
γ (deg)	77.71(2)
cell volume (Å^3)	2272(4)
Z	2
density (calcd)	1.385
absorb coeff (mm^{-1})	0.480
obsd no. of reflcns	16063
no. of unique reflcns ($I > 2\sigma$)	7346
GoF	1.011
R,[a] % [$I > 2\sigma$]	9.51
R_w,[a] % [$I > 2\sigma$]	15.12

[a] $R = \sum||F_o|-|F_c||/\sum|F_o|$. $R_w = \{\sum w(F_o^2 - F_c^2)^2/\sum w(F_o^2)^2\}^{1/2}$.

Copolymerizations Catalyzed by Cr(stmtaa)Cl (2) and Cr(s^{m}tmtaa)Cl (6). With the cocatalyst binding behavior of the strap (**2**) and strap mimic (**6**) complexes understood, the question of whether these complexes act as mono- or dicatalytic single-site catalysts for the epoxide/CO_2 copolymerization could finally be addressed. To reiterate the discussion vide supra, the strap moiety of

Figure 10. X-ray crystal structure of **2**, illustrating the ability of the chloride to bind within the cavity of the strap. Thermal ellipsoids are shown at the 50% probability level with hydrogens omitted for clarity.

complex **2** provides sufficient steric constraint to bind select cocatalysts to the underside of the metal center while complex **6** does not exhibit such selectivity. If these complexes are able to catalyze the copolymerization of cyclohexene oxide and carbon dioxide at a similar rate and produce copolymers with similar molecular weights and polydispersities, rationale would point to these complexes operating through the monocatalytic single-site pathway in which polymer chain propagation occurs

from only one side of the catalyst. To accurately investigate the ability of these complexes to polymerize cyclohexene oxide with carbon dioxide, both compounds were employed as catalysts under the same conditions utilized for copolymerizations using **1** discussed in previous reports.[21,22]

Table 4. Selected Bond and Contact Distances and Angles for **1** and **2**

	Cr(tmtaa)Cl (**1**)[a]	Cr(stmtaa)Cl·DMSO (**2**)
Cr−N1 (Å)	1.9881(18)	1.964(7)
Cr−N2 (Å)	1.9745(17)	1.984(7)
Cr−N3 (Å)	1.9900(18)	1.951(7)
Cr−N4 (Å)	1.9716(17)	1.985(8)
Cr−Cl (Å)	2.2607(7)	2.346(3)
Cr−O5 (Å)		2.033(5)
Cr−H29 (Å)		4.367
Cr−H30B (Å)		5.228
Cr−H36 (Å)		4.488
Cl−H29 (Å)		3.015
Cl−H30B (Å)		3.143
Cl−H36 (Å)		3.252
N1−Cr−N2 (deg)	92.98(7)	94.3(3)
N2−Cr−N3 (deg)	81.76(7)	84.7(3)
N3−Cr−N4 (deg)	92.96(7)	96.4(3)
N1−Cr−N4 (deg)	81.78(7)	84.3(3)
Cr−N_4 (Å)	0.4235	−0.0821

[a]Data taken from structure determination in ref 21.

The copolymerization reactions employing complexes **2** and **6** as catalysts were conducted in 20 mL of cyclohexene oxide, 2 equiv of PPNCl, and the appropriate amount of catalyst to achieve an M/I ratio ~1700. After the reaction mixture reached 80 °C, the reactor was charged with 35 bar CO_2 and allowed to react for a standard comparison time of 1 h. Figure 13 displays an overlay of the reaction profiles obtained from the copolymerization reactions, illustrating polycarbonate and cyclic carbonate production for both the strap and the strap mimic catalysts. It is easily seen from these profiles that formation of both polymer and cyclic carbonate occur at nearly identical rates for the two different catalyst systems. This leads to the assumption that the polymers were formed by the same mechanism. It follows from previous observations about the steric constraints of the strap moiety that chain growth must be occurring from only one side of the metal $-N_4$ plane. After the polymers were isolated and weighed, the TOFs were determined to be 807 h^{-1} for the strap catalyst (**2**) and 797 h^{-1} for the strap mimic catalyst (**6**). The ^1H NMR spectra of the purified polymers indicate

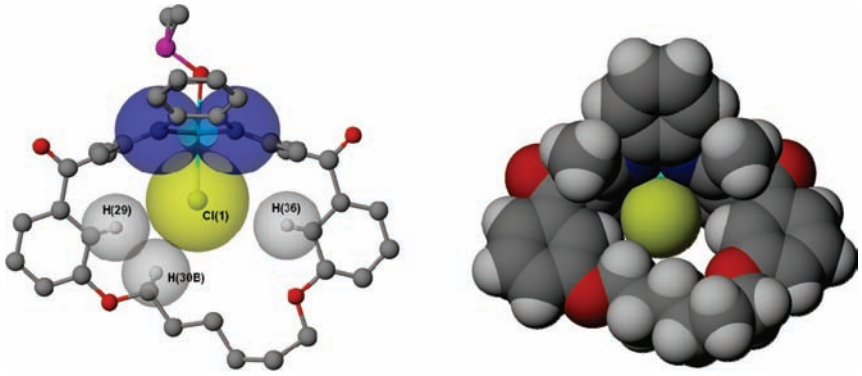

Figure 11. Three-dimensional representation from the X-ray crystal structure of **2**. The spheres represent the van der Waals radii of the selected atoms, illustrating the strict steric allowances of the strap moiety.

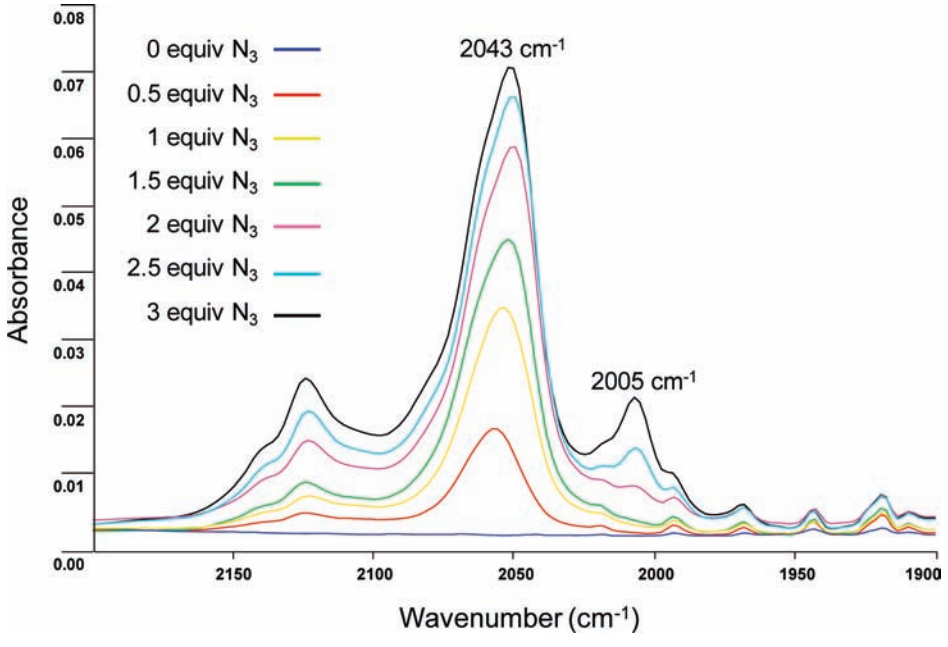

Figure 12. Infrared spectra from the titration of complex **6** with $PPNN_3$.

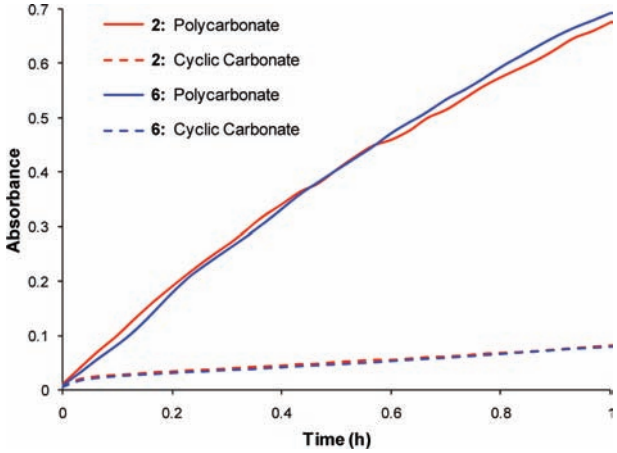

Figure 13. Reaction profiles indicating polycarbonate and cyclic carbonate formation with time for the copolymerization of cyclohexene oxide and CO_2, catalyzed by complexes **2** and **6** in the presence of 2 equiv of PPNCl and 35 bar carbon dioxide at 80 °C.

$>99\%$ CO_2 incorporation while the GPC profiles calculated number average molecular weights of 11,400 and 12,000 as well as polydispersity indices of 1.108 and 1.048 for **2** and **6**, respectively. The similarities in the quantities, properties of the isolated polymers, and the polydispersity indices further supports the theory of a mono catalytic single-site mechanism. These results, as well as other reaction parameters, are listed in Table 5 below.

Conclusions

In the interest of gaining insight into the mechanism of the copolymerization of epoxides with carbon dioxide, two new catalysts were developed based upon the chromium tetramethyltetraazaannulene system previously reported to be highly active and selective toward the production of poly (cyclohexylene carbonate).[21,22] These catalysts were designed to elucidate whether copolymer formation occurs from a single side of the metal $-N_4$ or two independent polymer chains were produced simultaneously. Previous efforts to address this ambiguity have focused on GPC analysis, where bimodal distributions where thought to be the result of two different active species, but findings were inconclusive as to whether the different molecular weight distributions were caused by dual catalysis at the active site or from chain termination caused by the presence of trace water during the reaction.[16−21] Reported herein is a different approach taken to address this mechanistic uncertainty, one that employs the concept of steric hindrance at the active site to control polymerization behavior. The first catalyst, Cr(stmtaa)Cl, contained a strap, tethering opposing sides of the complex and providing steric bulk under the metal center that limits polymer chain propagation to one side of the catalyst. Since the alterations to the complex would in turn alter the electronic environment around the chromium active site and make direct comparison to the parent complex, Cr(tmtaa)Cl, inapplicable, a similar catalyst, Cr(s^{m}tmtaa)Cl, with the same electronic features was designed to mimic the strapped complex while allowing the opportunity for dual-site catalysis to occur at a single metal center.

Table 5. Data Comparing the Results of the Copolymerizations of CHO and CO_2 for Catalysts **2** and **6**[a]

	Cr(stmtaa)Cl (**2**)	Cr(s^{m}tmtaa)Cl (**6**)
M/I	1709	1704
time (h)	1.0	1.0
polymer (g)	13.26	13.15
TON	806.6	797.3
TOF (h^{-1})	806.6	797.3
% CO_2[b]	$>99\%$	$>99\%$
M_n[c] ($g\cdot mol^{-1}$)	11,400	12,000
M_w[c] ($g\cdot mol^{-1}$)	12,700	12,600
PDI[d]	1.108	1.048

[a]Copolymerization reactions were conducted with 20 mL of CHO, 87 mg and 81 mg of **2** and **6**, respectively, and 2 equiv of PPNCl at 80 °C and under 35 bar CO_2 pressure for 1 h. [b]Determined by ^{1}H NMR. [c]Determined by GPC. [d]M_w/M_n.

The cavity on the underside of Cr(stmtaa)Cl created by the strap moiety was found to be large enough to accommodate the chloride anion, but too small to allow the azide anion to bind to the chromium center, while Cr(s^{m}tmtaa)Cl retained the ability to bind both the chloride and azide cocatalysts. This leads to the conclusion that the cavity of the strapped catalyst is large enough to allow binding of the cocatalyst, but too sterically encumbered to allow epoxide binding and polymerization to occur.

Both catalysts were able to copolymerize cyclohexene oxide and carbon dioxide to produce polymers with near identical reaction profiles and activities, achieving turnover frequencies of 807 h^{-1} and 797 h^{-1} for Cr(stmtaa)Cl (**2**) and Cr(s^{m}tmtaa)Cl (**6**), respectively. These copolymers produced also contained essentially indistinguishable molecular weights and molecular weight distributions of 11,400 $g\cdot mol^{-1}$ and 1.108 for Cr(stmtaa)Cl and 12,000 $g\cdot mol^{-1}$ and 1.048 for Cr(s^{m}tmtaa)Cl. Although the activities of these catalysts are, as expected based on electronic arguments, less than that of Cr(tmtaa)Cl, the copolymers contain molecular weight distributions that coincide exactly with copolymers obtained from the underivatized catalyst. Despite the observance of a slight shoulder in the higher molecular weight region of the GPC profiles, the infrared binding data, X-ray crystal structure, in situ infrared reaction profiles, and copolymer properties all support the conclusion that copolymerization of cyclohexene oxide with carbon dioxide occurs from only one side of the (tmtaa)CrCl catalyst via a mono catalytic single-site mechanism. *By analogy a similar occurrence is likely for (salen)MX and (porphyrin)MX catalyst systems.* Nevertheless, because these latter metal complexes are more planar than that of the saddle-shaped tetramethyltetraazaannulene complex, a *definitive* statement in these instances is not warranted.

Acknowledgment. We gratefully acknowledge the financial support from the National Science Foundation (CHE 05-43133) and the Robert A. Welch Foundation (A-0923).

Supporting Information Available: X-ray crystallographic files in CIF format for the structural determination of complex **2** and ligands **3**, **4**, and **5**. This material is available free of charge via the Internet at http://pubs.acs.org.